http://dx.doi.org/10.5012/bkcs.2013.34.7.2051

Theoretical Calculations of Infrared Bands of CH_3^+ and CH_5^+

Mohammad A. Matin, Joonkyung Jang,* and Seung Min Park†,*

*Department of Nanomaterials Engineering, Pusan National University, Miryang 627-706, Korea. *E-mail: jkjang@pusan.ac.kr*
*†Department of Chemistry and Research Center for New Nano Bio Fusion Technology, Kyung Hee University, Seoul 130-701, Korea. *E-mail: smpark@khu.ac.kr*
Received March 25, 2013, Accepted April 11, 2013

Existing theoretical calculations predict that infrared spectra of the two most fundamental reactive carbo-ions, methyl cation CH_3^+ with D_{3h} symmetry and protonated methyl cation CH_5^+ with C_s(I), C_s(II), and C_{2v} symmetries, appear together in the 7-μm region corresponding to the C-H bending modes. Vibrational band profiles of CH_3^+ and CH_5^+ have been compared by *ab initio* calculation methods that use the basis sets of MP2/aug-cc-pVTZ and CCSD(T)/cc-pVTZ. Our results indicate that the bands of rotation-vibration transitions of CH_3^+ and CH_5^+ should overlap not only in the 3-μm region corresponding to the C-H stretching modes but also in the 7-μm region corresponding to the C-H bending modes. Five band intensities of CH_5^+ among fifteen vibrational transitions between 6 and 8 μm region are stronger than those of the ν_2 and ν_4 bands in CH_3^+. Ultimate near degeneracy of the two bending vibrations ν_2 and ν_4 of CH_3^+ along with the stronger intensities of CH_5^+ in the three hydrogen scrambling structures may cause extreme complications in the analysis of the high-resolution carbo-ion spectra in the 7-μm region.

Key Words : *Ab initio* calculations, Vibrational frequencies, Infrared spectra, CH_3^+, CH_5^+

Introduction

The observation of carbo-ions in space will also help the understanding of chemistry in many astronomical objects.[1,2] The methyl cation CH_3^+ is the most important reactive species in organic, combustion, atmospheric, and interstellar chemistry.[3] There have been a number of laboratory spectroscopic studies on carbo-ions in the last few decades. Many interesting fundamental carbo-cations such as CH_2^+ and CH_3^+ have been observed and analyzed using high-resolution infrared laser spectroscopic techniques.[4-6] Subsequent spectroscopic and chemical dynamics studies of the CH_5^+ carbo-cation are reported.[7-9] The information on the quantum mechanical property of CH_3^+ was obtained from the previous spectroscopic studies.[5,10-12] Theoretical calculations[13,14] have also reported that the two vibrational states of CH_3^+ lie quite close to each other. The determination of vibrational frequencies by computational methods has become increasingly important in many areas in chemistry. Protonated methyl cation (CH_5^+) is one of the important reactive species in combustion, atmospheric, and interstellar chemistry. High-resolution infrared spectrum of CH_5^+ corresponding to the C-H stretching band in the 3.4 μm region was reported.[7] This cation is also of great basic interest because it is known to be highly fluxional: that is, the five protons are equivalent and can exchange freely. Early theoretical investigations of the electronic structure of CH_5^+ suggested it might consist of pyramidal CH_3^+ subunit bound to an H_2 molecule, in a C_s symmetric arrangement. But it has other two low energy structures C_s(II) and C_{2v} symmetric structure with almost no barrier. Recent theoretical investigations of CH_5^+ have been performed to understand the dynamics and infrared spectrum of CH_5^+.[9,15] Despite the plausible identity of CH_3^+, it is possible that some of the spectral lines are due to CH_5^+. Here, we have calculated the harmonic vibrational frequencies of CH_3^+ and the three C_s(I), C_s(II), and C_{2v} structures of CH_5^+ along with their relative intensities at different theoretical levels. We provide the theoretical calculations of the vibrational spectra for CH_3^+ and CH_5^+ in the infrared region to facilitate the detection of this carbo-ion in interstellar space and have hindsight to analyze their high-resolution spectral analysis in the 7-μm region corresponding to the C-H bending modes.

Computational Details

By using Gaussian 09 package,[16] we have optimized the geometries and calculated vibrational frequencies of CH_3^+ and CH_5^+ by using *ab initio* quantum mechanical methods and density functional theory (DFT) methods. Harmonic vibrational frequencies were determined by the analytical evaluation of the second derivative of the energy with respect to nuclear displacement. The *ab initio* calculations were performed at the levels of MP2/aug-cc-pVTZ and CCSD(T)/cc-pVTZ with an analytic gradient to optimize geometries and calculate frequencies for CH_3^+ and CH_5^+. We used the numeric second derivatives of energy for calculating frequencies at the level of CCSD(T). Geometry optimization was taken to be converged if the maximal atomic force was smaller than 0.00045 Hartree $Bohr^{-1}$. We also tried various levels of theory, such as B3LYP/6-311G(d,p) and QCISD/aug-cc-pVTZ. See the Supporting Information for the results from HF, MP2, QCISD, CCSD, CCSD(T), and B3LYP.

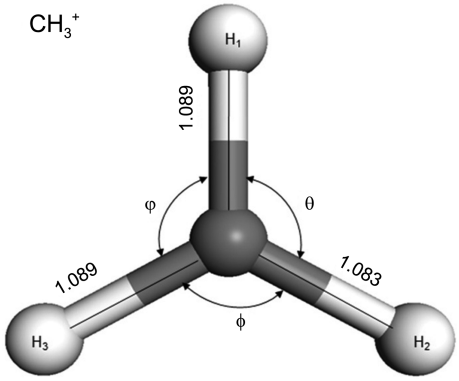

Figure 1. Optimized structure and geometrical parameters of CH_3^+ calculated at the CCSD(T)/cc-pVTZ level of theory.

Results and Discussions

The structure of CH_3^+ optimized with CCSD(T)/cc-pVTZ is shown in Figure 1. The structural parameters defined in Figure 1 are listed in Table 1. The C–H bond distances of CH_3^+ were calculated to be R_1 = 1.089, R_2 = 1.083, and R_3 = 1.089 Å, respectively. The present geometry of CH_3^+ agrees well with the result of Crofton *et al.* (1.087 Å).[5] Also shown in Table 1 are the results calculated by the MP2/aug-cc-pVTZ method. The MP2 results are not much different from the CCSD(T) results.

In Figure 2, we show three optimized (CCSD(T)/cc-pVTZ) structures of CH_5^+ with symmetries C_s(I), C_s(II), and C_{2v}. The C_s(I) structure is the energy minimum structure, and the other two structures correspond to saddle points. Our calculation is in agreement with those[17] computed at the CCSD (T)/aug-cc-pVTZ level of theory. For the C_s(I) structure, the bond distances are R_1 = 1.198, R_2 = 1.198, R_3 = 1.104, and R_4 and R_5 = 1.086 Å (Table 1). The distance of two H atoms is 0.940 Å. The bond distances of the C_s(II) structure are R_1 = 1.200, R_2 = 1.200, R_3 = 1.082, and R_4 and R_5 = 1.096 Å; the distance of the two H atoms is 0.933 Å. The bond distances of the C_{2v} structure are R_1 = 1.139, R_2 = 1.160, R_3 and R_5 = 1.085, and R_4 = 1.139 Å; the bond distance of the two H atoms is R_6 = 1.174 Å. The distances of two of the H atoms from the carbon atom are slightly greater than the other two structures.

Having confirmed that the present calculation yields geometries reasonably consistent with the previous experiments and theoretical reports, we moved on to predictions of harmonic vibrational frequencies of both CH_3^+ and the C_s(I), C_s(II), and C_{2v} structures of CH_5^+ at both MP2/aug-cc-pVTZ and CCSD(T)/cc-pVTZ levels. The calculated frequencies are listed for CH_3^+ and CH_5^+ in Tables 2 and 3, respectively.

Table 2 shows the present MP2/aug-cc-pVTZ calculation accords with the experimental vibrational frequencies of

Table 1. Optimized geometrical parameters for CH_5^+ (CCSD(T)/cc-pVTZ) and CH_3 (CCSD(T)/cc-pVTZ) (bond lengths, rs, and angles are in Å and degrees, respectively)

	CH_3^+	CH_5^+					
		C_s(I)	C_s(II)	C_{2v}	[d]C_s(I)	[d]C_s(II)	[d]C_{2v}
$r(C\text{-}H_1)=R_1$	1.089(1.0864[a])	1.198(1.182[b])	1.200(1.187[b])	1.139(1.138[b])	1.197	1.200	1.163
$r(C\text{-}H_2)=R_2$	1.083(1.0864[a])	1.198(1.183[b])	1.200(1.187[b])	1.160(1.160[b])	1.197	1.200	1.087
$r(C\text{-}H_3)=R_3$	1.089(1.0864[a])	1.104(1.087[b])	1.082(1.081[b])	1.085(1.084[b])	1.108	1.084	1.142
$r(C\text{-}H_1)=R_4$		1.086(1.085[b])	1.096(1.097[b])	1.139(1.138[b])	1.088		
$r(C\text{-}H_5)=R_5$		1.086(1.085[b])	1.096(1.097[b])	1.085(1.084[b])			
$r(H_1\text{-}H_2)=R_6$		0.940(0.975[b])	0.933(0.962[b])	1.174(1.174[b])	0.952	0.945	
θ	120.02(120.00[a])	45.8(48.7[b])	45.7(47.8[b])	122.8(123.2[b])			
ϕ	119.08(120.00[a])	119.1(119.7[b])	106.3(105.1[b])	119.0(122.1[b])			
φ	119.98(119.98[a])						
Expt.	1.087[c]						

[a,b]Calculated at the MP2/aug-cc-pVTZ level. [c]From reference 5. [d]From reference 17.

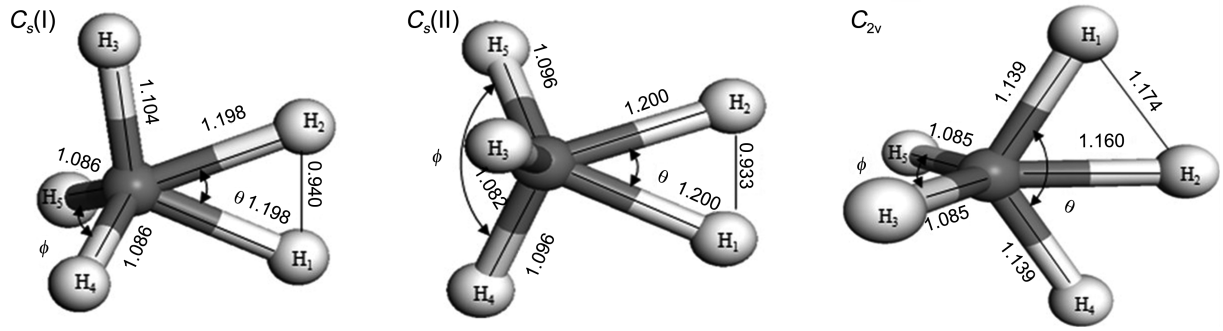

Figure 2. Optimized structures and geometrical parameters of CH_5^+ calculated at the CCSD(T)/cc-pVTZ level of theory. Three structures of CH_5^+, denoted as C_s(I), C_s(II), and C_{2v}, are shown.

Table 2. Theoretical predictions of Harmonic Vibrational Frequencies of CH_3^+ (in cm^{-1}) at MP2/aug-cc-pVTZ and CCSD(T)/cc-pVTZ level of theory

Basis sets	Frequency (cm^{-1})				Scale factor
	ν_1	ν_2	ν_3	ν_4	
MP2/aug-cc-pVTZ	2915.4	1360.2	3109.1	1367.6	0.9437
[a]Reference values (MP2/aug-cc-pVTZ)	2917.9	1360.2	3108.4	1365.3	
CCSD(T)/cc-pVTZ	2939.5	1402.3	3131.2	1400.6	0.9748
[b]Reference values CCSD(T)/aug-cc-pVTZ	3039.3	1429.0	3236.9	1421.6	
Expt.		1380 ± 20[c]	3108.4[d]		

[a]From reference 18. [b]From reference 17. [c]From reference 11. [d]From reference 5.

Table 3. Theoretical predictions of Harmonic Vibrational Frequencies of CH_5^+ (in cm^{-1}) at the global minimum C_s(I) and C_s(II) and C_{2v} geometries at the MP2/aug-cc-pVTZ and CCSD(T)/cc-pVTZ level of theory

Symmetry Mode[a]	C_s(I)		C_s(II)		C_{2v}	
	MP2/aug-cc-pVTZ[b]	CCSD(T)/cc-pVTZ[c]	MP2/aug-cc-pVTZ[b]	CCSD(T)/cc-pVTZ[c]	MP2/aug-cc-pVTZ[b]	CCSD(T)/cc-pVTZ[c]
1	254	196	228*i*	188*i*	589*i*	676*i*
2	750	846	957	1013	488	498
3	1288	1283	1139	1159	1256	1240
4	1302	1295	1331	1342	1320	1313
5	1472	1464	1479	1482	1414	1402
6	1502	1480	1504	1502	1452	1446
7	1583	1551	1611	1630	1480	1467
8	2516	2489	2483	2414	2673	2645
9	2715	2684	2730	2777	2737	2706
10	3029	2988	3073	3071	2898	2865
11	3165	3120	3132	3130	3163	3116
12	3266	3218	3277	3255	3280	3228

[a]The normal modes are numbered in order of increasing frequency. [b]Scale factor for MP2/aug-cc-pVTZ = 0.9437. [c]Scale factor for CCSD(T)/cc-pVTZ = 0.9748

CH_3^+. The ν_2 frequency deviates by less than 1.43% from the experimental value, whereas the ν_3 position lies 0.02% above the experimental value. At a higher level of theory, CCSD(T), the experimental data are consistent with theoretical calculations. At the CCSD(T)/cc-pVTZ level, the deviation of the ν_2 frequency is 1.62% above the experimental value and the ν_3 position is 0.73% above the experimental value. Our finding is consistent with the previous report that MP2 theory agrees with experiment better than CCSD(T) theory.[17,18]

We calculated harmonic vibrational frequencies of CH_5^+ with structures of C_s(I), C_s(II), and C_{2v} symmetries at the MP2/aug-cc-pVTZ and CCSD(T)/cc-pVTZ levels (Table 3). Note that the minimum C_s(I) structure has all the real frequencies, whereas both the C_s(II) and C_{2v} structures have one imaginary frequency because they are saddle-point structures. From the normal mode analysis, the C_s(II) structure is found to be at the saddle point for H_2 rotation about the C_3 axis of the CH_3 moiety of CH_5^+. The C_{2v} structure corresponds to a saddle point for the structural change of $C_s(I) \rightarrow C_{2v} \rightarrow C_s(I)$. The calculated frequencies are in agreement with the previous results.[17,19]

Quantitative prediction by using the *ab initio* method for the intensities associated with infrared spectra of molecules is particularly difficult to achieve. Reliable theoretical estimates of infrared intensities can be expected from computations that provide an accurate description of the electronic charge density and its dynamics with vibrational distortions. It should be emphasized that the simultaneous theoretical prediction of vibrational frequencies and infrared intensities may be considered as an important criterion for accuracy.

We analyzed the infrared spectra of CH_3^+ and CH_5^+ in the range of 0-3300 cm^{-1} at the CCSD(T)/cc-pVTZ level of theory (Figure 3). The calculated position of the ν_3 asymmetric stretching vibration in CH_3^+ is located at 3131.2 cm^{-1} (upper). The calculated spectra of CH_5^+ compare well with a low-resolution experimental spectrum except below 1000 cm^{-1} where the experimental spectrum shows no absorption.[9] Our calculations find substantial absorption features below 1000 cm^{-1}. Below 1000 cm^{-1}, known as a low-temperature nonscrambling regime, protons forming the H_2 moiety and those engaged in the CH_3 tripod lead to two well-separated stretching peaks (Figure 3, upper panel). The theoretically observed infrared spectrum clearly indicates full hydrogen scrambling of CH_5^+.

In Figure 3, the ν_3 band origin[5] in CH_3^+ was fixed to 3108 cm^{-1}. The band intensities of ν_2 and ν_4 in CH_3^+ are calculated to be weaker by a factor of 6.64 and 4.26, respectively,

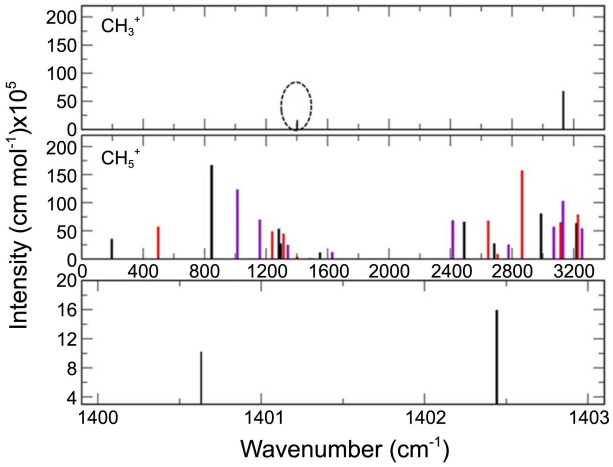

Figure 3. Infrared spectrum for CH_3^+ (upper panel) and three structures C_s(I) (black), C_s(II) (violet), and C_{2v} (red) of CH_5^+ (middle panel) at the CCSD(T)/cc-pVTZ level of theory. Shown in the bottom is the enlarged CH_3^+ spectrum in the range of 1400.0 to 1403 cm^{-1} (denoted as a circle in the upper panel).

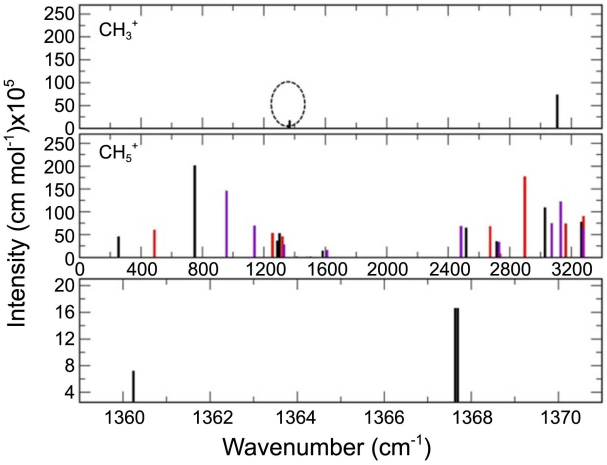

Figure 4. Infrared spectra at the MP2/aug-cc-pVTZ level of theory.

than that of the ν_3 band at the CCSD(T)/cc-pVTZ level of theory. At the MP2/aug-cc-pVTZ level, these intensity difference factors increase to 10.2 and 4.39, respectively. On the other hand, for CH_5^+, at the CCSD(T)/cc-pVTZ level of theory, the strongest CH_5^+ band positions are located at 2988, 3071, and 2865 cm^{-1} for the C_s(I), C_s(II), and C_{2v} structures near to 2950 cm^{-1}, as seen in the experimental observation.[7] The three strongest band positions are calculated at 3029, 3132, and 2898 cm^{-1} using the MP2/aug-cc-pVTZ level. There are all together 14 (5, 4, and 5 from the C_s(I), C_s(II), and C_{2v} structures, respectively) vibrational bands of CH_5^+ between 1200 and 1650 cm^{-1} (8.06 to 6.06 μm) from the two calculation results. Among the 14 transitions, the five vibrational band intensities of CH_5^+ are predicted to be stronger than that of the ν_4 band in CH_3^+.

We calculated the theoretical spectra for CH_3^+ and CH_5^+ at the MP2/aug-cc-pVTZ level (Figure 4). The theoretical spectra are not much different from those obtained by using CCSD(T)/cc-pVTZ. It is noteworthy that the infrared intensities of CH_3^+ and CH_5^+ appear to be in the 3-μm region, as estimated in the previous report,[7] whereas most CH_5^+ vibrational modes are predicted to be stronger than the two ν_2 and ν_4 vibrational modes of CH_3^+. Also, it should be mentioned that the ν_4 intensity is calculated to be consistently stronger by a factor of 2 than that of the ν_2 band at the two levels of the calculations.

Figures 3 and 4 indicate that there is a greater possibility that CH_5^+ lines are found in the 7-μm region as well as those from CH_3^+. We also point out that the rotational constants of the two carbo-cations due to their small molecular weights are large enough to spread out their rotation-vibration transitions in a wide wavelength region.

Conclusion

By using quantum mechanical calculations, we predicted the infrared spectra of the two most fundamental reactive carbo-ions, methyl cation CH_3^+ with D_{3h} symmetry and protonated methyl cation CH_5^+ with C_s(I), C_s(II), and C_{2v} symmetries. The calculated results indicate that the rotation-vibration band transitions of CH_3^+ and CH_5^+ should overlap not only in the 3-μm region corresponding to the C-H stretching modes but also in the 7-μm region corresponding to the C-H bending modes. Five band intensities of CH_5^+ among fifteen vibrational transitions between 6 and 8 μm region are stronger than those of the ν_2 and ν_4 bands in CH_3^+. Ultimate near degeneracy of the two bending vibrations ν_2 and ν_4 of CH_3^+ along with the stronger intensities of CH_5^+ in the three hydrogen scrambling structures may cause extreme complications in the analysis of the high-resolution carbo-ion spectra in the 7-μm region.

Acknowledgments. This work is supported by the National Research Foundation (2012-047626 and 2012-000484).

References

1. Herbst, E.; Klemperer, W. *Astrophys. J.* **1973**, *185*, 505.
2. Geballe, T. R.; Oka, T. *Nature* **1996**, *384*, 334.
3. Smith, D. *Phil. Trans. R. Soc. Lond., A* **1987**, *323*, 269.
4. Rösslein, M.; Gabrys, C. M.; Jagod, M.-F.; Oka, T. *J. Mol. Spectrosc.* **1992**, *153*, 738.
5. Crofton, M. W.; Jagod, M.-F.; Rehfuss, B. D.; Kreiner, W. A.; Oka, T. *J. Chem. Phys.* **1988**, *88*, 666.
6. Jagod, M.-F.; Gabrys, C. M.; Rösslein, M.; Uy, D.; Oka, T. *Can. J. Phys.* **1994**, *72*, 1192.
7. White, E. T.; Tang, J.; Oka, T. *Science* **1999**, *284*, 135.
8. Asvany, O.; Kumar, P.; Redlich, P. B.; Hegemann, I.; Schlemmer, S.; Marx, D. *Science* **2005**, *309*, 1219.
9. Huang, X.; McCoy, A. B.; Bowman, J. M.; Johnson, L. M.; Savage, C.; Dong, F.; Nesbitt, D. J. *Science* **2006**, *311*, 60.
10. Herzberg, G.; Shoosmith, J. *Can. J. Phys.* **1956**, *34*, 523.
11. Dyke, J.; Jonathan, N.; Lee, E.; Morris, A. *J. Chem. Soc. Faraday Trans. II* **1976**, *72*, 1385.
12. Liu, X.; Gross, R. L.; Suits, A. G. *Science* **2001**, *294*, 2527.
13. Yua, H.-G.; Sears, T. J. *J. Chem. Phys.* **2002**, *117*, 666.
14. Cunha de Miranda, B. K.; Alcaraz, C.; Elhanine, M.; Noller, B.;

Hemberger, P.; Fischer, I.; Garcia, G. A.; Soldi-Lose, H.; Gans, B.; Mendes, L. A.; Boyé-Péronne, S.; Douin, S.; Zabka, J.; Botschwina, P. *J. Phys. Chem. A* **2010**, *114*, 4818.
15. Hinkle, C. E.; McCoy, A. B. *J. Phys. Chem. A* **2012**, *116*, 4687.
16. Frisch, M. J.; Trucks, G. W.; Schlegel, H. B.; Scuseria, G. E.; Robb, M. A.; Cheeseman, J. R.; Scalmani, G.; Barone, V.; Mennucci, B.; Petersson, G. A.; Nakatsuji, H.; Caricato, M.; Li, X.; Hratchian, H. P.; Izmaylov, A. F.; Bloino, J.; Zheng, G.; Sonnenberg, J. L.; Hada, M.; Ehara, M.; Toyota, K.; Fukuda, R.; Hasegawa, J.; Ishida, M.; Nakajima, T.; Honda, Y.; Kitao, O.; Nakai, H.; Vreven, T.; Montgomery, J. A., Jr.; Peralta, J. E.; Ogliaro, F.; Bearpark, M.; Heyd, J. J.; Brothers, E.; Kudin, K. N.; Staroverov, V. N.; Kobayashi, R.; Normand, J.; Raghavachari, K.; Rendell, A.; Burant, J. C.; Iyengar, S. S.; Tomasi, J.; Cossi, M.; Rega, N.; Millam, J. M.; Klene, M.; Knox, J. E.; Cross, J. B.; Bakken, V.; Adamo, C.; Jaramillo, J.; Gomperts, R.; Stratmann, R. E.; Yazyev, O.; Austin, A. J.; Cammi, R.; Pomelli, C.; Ochterski, J. W.; Martin, R. L.; Morokuma, K.; Zakrzewski, V. G.; Voth, G. A.; Salvador, P.; Dannenberg, J. J.; Dapprich, S.; Daniels, A. D.; Farkas, Ö.; Foresman, J. B.; Ortiz, J. V.; Cioslowski, J.; Fox, D. J. *Gaussian 09*, revision B.02; Gaussian, Inc.: Wallingford, CT, 2010.
17. Jin, Z.; Braams, B. J.; Bowman, J. M. *J. Phys. Chem. A* **2006**, *110*, 1569.
18. Olkhov, R. V.; Nizkorodov, S. A.; Dopfer, O. *J. Chem. Phys.* **1999**, *110*, 9527.
19. Brown, A.; McCoy, A. B.; Braams, B. J.; Jin, Z.; Bowman, J. M. *J. Chem. Phys.* **2004**, *121*, 4105.